

## ***Interactive comment on “Local time extent of magnetopause reconnection X-lines using space–ground coordination” by Ying Zou et al.***

**Ying Zou et al.**

yingzou@bu.edu

Received and published: 27 September 2018

This manuscript uses a combination of satellite and ground-based radar data to estimate the spatial extent of magnetopause reconnection for 3 example events. The motivation for the study is very good and the results are potentially interesting and important but, in my view, the crucial radar analysis falls short of the state of the art and needs improving to support the interpretation. Even if this does not radically change the main results, it would put the results on a sounder footing, better evaluate sources and sizes of uncertainties, and allow the results given here to be compared more objectively to past and future studies. For this reason, I would not recommend publication in its present form. My recommendations are as follows: 1. Follow the state of the art in the current analysis, evidence for the reconnection X-line is essentially based on looking

C1

for high-speed flows in the vicinity of a high radar spectral width region (e.g., Figure 2a-d) and the X-line extent is estimated from a longitudinal profile of northward velocity at a relatively arbitrary magnetic latitude. In my view this is a rather crude analysis and it should be possible to do this better by estimating the profile of the reconnection electric field itself along the open-closed field line boundary (OCB) and its time evolution following the methodology set out in detail in: Chisham, G., et al. (2008), Remote sensing of the spatial and temporal structure of magnetopause and magnetotail reconnection from the ionosphere, *Rev. Geophys.*, 46, RG1004, doi:10.1029/2007RG000223. Freeman, M. P., G. Chisham, and I. J. Coleman (2007), Remote sensing of reconnection, in *Reconnection of Magnetic Fields*, edited by J. Birn and E. Priest, chap. 4.6, pp. 217–228, Cambridge Univ. Press, New York. In essence, this method requires the following steps: a. Identify the OCB objectively at as many locations as possible using available datasets and interpolate in space and time where necessary using suitable models, e.g., figures 6, 8, 9, 11 in Chisham et al (2008). b. Estimate the reconnection electric field along the OCB by measuring the electric field component parallel to the boundary (or  $E \times B$  velocity component perpendicular to it) in the rest frame of the generally moving boundary, e.g., figure 13 in Chisham et al. (2008). c. Plot profiles of the reconnection electric field versus MLT over the time interval of interest. Use the zero crossing locations of these profiles to estimate the MLT extent of reconnection as a function of time, e.g., figure 7 of Pinnock et al., (2003), The location and rate of dayside reconnection during an interval of southward interplanetary magnetic field, *Ann. Geophys.*, 21, 1467–1482. d. Project the MLT extent to the magnetopause using a suitable model to estimate the X-line length and its evolution and to compare with in-situ spacecraft observations of presence or absence of reconnection, e.g., figure 8 of Pinnock et al. (2003). The authors' analysis is only a very crude approximation to this. Particular areas of improvement that I would recommend include:

Response: We thank the reviewer for the detailed comments and instructions. We realize that our view of “X-line” is different from the reviewer's and this seems to have affected the understanding of how an X-line extent should be measured. In our original

C2

terminology we used “magnetic separator” to refer to the global configuration along which reconnection occurs at various rates, and used “X-lines” to refer to regions of strong reconnection, i.e., reconnection bursts, which could activate over a segment of the magnetic separator. The focus of the paper is the latter, as motivated by progresses in recent numerical simulations [Shay et al., 2003; Sheperd and Cassak, 2012]. To avoid confusion, we replace “extent of X-lines” with “extent of reconnection bursts”.

The references of X-line extent given by the reviewer provide valuable groundwork of clarifying the scope of this study. We rewrote the first paragraph as “. . .Reconnection tends to occur at sites of strictly anti-parallel magnetic fields as anti-parallel reconnection [e.g. Crooker, 1979; Luhmann et al., 1984], or occur along a line passing through the subsolar region as component reconnection [e.g. Sonnerup, 1974; Gonzalez and Mozer, 1974]. Evidence shows either or both can occur at the magnetopause and the overall reconnection extent can span from a few up to 40 Re [Paschmann et al., 1986; Gosling et al., 1990; Phan and Paschmann, 1996; Coleman et al., 2001; Phan et al., 2001, 2003; Chisham et al., 2002, 2004, 2008; Petrinec and Fuselier, 2003; Fuselier et al., 2002, 2003, 2005, 2010; Petrinec and Fuselier, 2003; Pinnock et al., 2003; Bobra et al., 2004; Trattner et al., 2004, 2007, 2008, 2017; Trenchi et al., 2008]. However, reconnection does not occur uniformly across this configuration but has spatial variations [Pinnock et al., 2003; Chisham et al., 2008]. The local time extent of reconnection bursts is the focus of this study.”

The methodology adopted by our paper has been commonly used for studying reconnection bursts. It is a common approach to measure the flow extent at a latitude poleward of the OCB as the reconnection extent [Goertz et al., 1985; Pinnock et al., 1993, 1995; Provan and Yeoman, 1999; Thorolfsson et al., 2000; McWilliams et al., 2001a, 2001b; Elphic et al., 1990; Denig et al., 1993; Neudegg et al., 1999, 2000; Lockwood et al., 2001; Wild et al., 2001, 2003, 2007; McWilliams et al., 2004; Zhang et al., 2008]. Based on the snapshots the flow extent did not change much over a 2-3° displacement in latitude. Considering these numerous past works, methodology has

C3

followed a standard approach.

However, we appreciate the reviewer’s suggestion and think that it is a good idea to compare our flow velocity profile with the reconnection electric field profile derived following Pinnock et al. [2003], Freeman et al. [2007], Chisham et al. [2008]. We have followed the helpful instructions given by the reviewer and presented our result in Figure S3 based on event #1 (replaced with a new event following the advice of reviewer #1). Details can be found below.

2. Improved estimates of the OCB (step 1a above) a. The authors use a 150 m/s spectral width threshold to estimate the OCB but then apply it rather vaguely by drawing a red contour in figures 2d, 4d, 6d which doesn’t match the 150 m/s threshold everywhere. The authors then largely ignore this anyway by using examining the ExB velocity on a fixed latitude circle that is generally poleward of where they say the OCB is. For example, for the first event in section 3.1.2, in lines 293-295 it is said that the OCB is at 77 deg latitude based on the spectral width in figure 2d but in lines 360-366 the 80 deg latitude circle is used as the OCB for the velocity cross-section shown in figure 2f. Similarly, in section 3.2.2, it is 77 deg latitude (lines 390-391) from figure 4d and 79 deg latitude (figure 4 caption) used for figure 4f. And in section 3.2.2, it is 80 deg latitude (figure 6 caption) used for figure 6g,h but the spectral width boundary is unstated and appears to be at lower latitude (at about the projected THA position). b. According to the following references it should be possible to estimate the OCB from spectral widths at a wide range of local times using the method of Chisham and Freeman (2004) and I recommend that this be attempted more carefully and objectively. Chisham, G., and M. P. Freeman (2003), A technique for accurately determining the cusp-region polar cap boundary using SuperDARN HF radar measurements, *Ann. Geophys.*, 21, 983–996. Chisham, G., and M. P. Freeman (2004), An investigation of latitudinal transitions in the SuperDARN Doppler spectral width parameter at different magnetic local times, *Ann. Geophys.*, 22, 1187–1202. Chisham, G., M. P. Freeman, and T. Sotirelis (2004a), A statistical comparison of SuperDARN spectral width

C4

boundaries and DMSP particle precipitation boundaries in the nightside ionosphere, *Geophys. Res. Lett.*, 31, L02804, doi:10.1029/2003GL019074. Chisham, G., M. P. Freeman, T. Sotirelis, R. A. Greenwald, M. Lester, and J.-P. Villain (2005a), A statistical comparison of SuperDARN spectral width boundaries and DMSP particle precipitation boundaries in the morning sector ionosphere, *Ann. Geophys.*, 23, 733–743. Chisham, G., M. P. Freeman, T. Sotirelis, and R. A. Greenwald (2005b), The accuracy of using the spectral width boundary measured in off-meridional SuperDARN HF radar beams as a proxy for the open-closed field line boundary, *Ann. Geophys.*, 23, 2599–2604. Chisham, G., M. P. Freeman, M. M. Lam, G. A. Abel, T. Sotirelis, R. A. Greenwald, and M. Lester (2005c), A statistical comparison of SuperDARN spectral width boundaries and DMSP particle precipitation boundaries in the afternoon sector ionosphere, *Ann. Geophys.*, 23, 3645–3654. c. The OCB can also be estimated from other data, such as DMSP particle precipitation. It seems that this data might be available for the events studied, see <https://heliophysicsdata.sci.gsfc.nasa.gov/websearch/dispatcher> Even if not particularly close in MLT or UT it may be useful as a constraint. d. The T89 model projections of the THA magnetopause crossing to the ionosphere in Figures 4 and 6 appear to agree with the OCB location estimated from the spectral width. It would thus seem reasonable to use the model to estimate the OCB location in the ionosphere at all dayside MLT at this UT. The projected location of THE may be different in these two cases because from Figure 3 there is evidently a rapid outward expansion of the magnetopause from 9.4 RE to 10.2 RE between 1826 and 1828 UT which would need appropriate re-scaling of the model to capture, and in Figure 5 the spacecraft are separated by over 30 min in time and so again the model conditions are probably different. In these cases, and for the figure 2 event, it seems reasonable to explore simple scalings of the T89 model that would fit the magnetopause crossing location of each spacecraft and see if this improves the projected location of the spacecraft with respect to the spectral width boundary. If so, then the model could be used to extrapolate to all dayside MLT. e. Alternatively, a simple offset circle model is commonly a good approximation to the OCB, whose free parameters could be constrained by spectral width and

C5

possibly DMSP data. This would at least be an improvement on assuming a latitudinal circle that is rather unrelated to the spectral width boundary. In all of the above cases, limitations and assumptions can be assessed by error and sensitivity analyses. For example, how are the results 1b-d above affected by changing the inferred boundary by 1 degree say?

Response: Figures S3a-c present the OCB of event #1 around the space-ground conjunction time and longitude. We have identified the OCB more precisely following Chisham and Freeman [2003, 2004] and Chisham et al. [2004, 2005a, 2005b, 2005c] and it is drawn as the dashed black line. The OCB in this event was found nearly along a constant latitude. THEMIS satellite footprints were mapped very closely to the OCB.

3. Take account of the generally moving OCB (step 1b above) As emphasised in the references in 1 above, the reconnection rate is the electric field in the frame of the moving OCB and this can sometimes affect the inference of whether reconnection is occurring or not, e.g., see Figure 13 of Chisham et al. (2008). Some account of this should be taken in the present analysis as it may affect the edges of the inferred reconnection region in particular and hence the FWHM.

Response: Figures S3d-f present time series of the spectral width measurements along beams 4, 7, and 10, as a function of latitude. The time series plot allows us to determine the speed of the OCB motion and we determined the speed at each individual beam. Note that the OCB motion was longitudinally dependent and was faster around eastern than western beams.

4. Project the ExB velocity perpendicular to the boundary (relevant to step 1c above) Given the strong rotation of the flow seen in figure 2 in particular, consideration should be given of the effect of uncertainties in the assumed orientation of the OCB on the projected flow component across it as this could change the inferred X-line extent.

Response: Figure S3g presents the electric field along the OCB in the frame of the ionosphere (dotted), and in the frame of the OCB (solid). The latter is the reconnection

C6

electric field. The reconnection electric field had essentially the same FWHM as the flow slightly poleward of the OCB (difference being less than the radar spatial resolution). Although the method suggested by the reviewer has its advantage, we note that the process of tracking OCB motion can introduce large uncertainties, especially for our events where the OCB moved very slowly (Figure S1). Given the radar spatial ( $\sim 0.3^\circ$ ) and temporal (2 min) resolution, the speed of OCB has an uncertainty of  $\sim 300$  m/s. This results in a signal to noise ratio generally around or even below 1 for the OCB speed, even though we have not yet considered the measurement error associated with spectral widths or the error of using 150 m/s as the OCB threshold in any given event. A similarly poor signal to noise ratio has been found in Chisham et al. [2008]. This would affect the estimate of the electric field and would reduce the confidence of the results. Therefore it is not entirely clear to us whether deriving the reconnection electric field serves as a better methodology for the purpose of our study.

Our study does not discuss the magnitude of the reconnection electric field, but the width is the focus. The flow velocity poleward of the OCB is less affected by the OCB uncertainties. Given that the electric field profiles at the OCB latitude and the flow velocity profile slightly poleward are about the same, that the echoes are more continuous at higher latitudes, and that our approach is consistent with a number of past works cited above, we think that our approach is sufficient to lead to the conclusion.

The above discussion has been clarified in the text as "It is noteworthy mentioning that the velocity profile obtained above approximates to the profile of reconnection electric field along the open-closed field line boundary (details in Figure S3). Reconnection electric field can be estimated by measuring the flow across the open-closed field line boundary in the reference frame of the boundary [Pinnock et al., 2003; Freeman et al., 2007; Chisham et al., 2008]. However, a precise determination of the boundary motion is subject to radar spatial and temporal resolution and for a slow motion like events studied in this paper (Figure S1), the signal to noise ratio is lower than one. For this reason this paper focuses on the velocity profile poleward of the open-closed field

C7

line boundary, which is less affected by the error associated with the boundary. " We did not consider the OCB location beyond the radar FOV because this study is about flows in the satellite-ground conjunction region (not the entire X-line extent). Since the flow FWHM is confined in the radar FOV, our conclusion does not rely on flow or OCB outside the radar FOV.

5. Improved consideration of the temporal evolution The current analyses are strongly biased towards comparisons of magnetopause and ionospheric observations of reconnection at a common instant. Given the uncertainties in how reconnection may evolve at the magnetopause, and the ionospheric response times, it would be helpful to repeat the analysis shown in figure 2f, 4f, and 6g,h at some sampling frequency throughout the intervals shown in figures 2e, 4e, and 6e,f. The temporal evolution of  $I_{os}$  data shown in figures 2e, 4e, and 6e,f are a rather poor proxy by which to estimate the evolution of X-line extent and something similar to figure 7 of Pinnock et al (2003) would be very interesting to see, especially for the inferred complex evolution of the Apr 29 event.

Response: As clarified above, we target reconnection bursts whose extent is by convention measured as the ionospheric flow width. We also focus on the times of satellite magnetopause crossings in order to achieve a space-ground comparison.

6. Discrepancies in magnetopause to ionosphere projection (step 1d above) The magnetopause crossings of spacecraft THA and THD in figure 2, and THE in figure 4 (and possibly figure 6 too) project several degrees of latitude away from the expected OCB location based on spectral width. This suggests that the estimation of X-line extent at the magnetopause from that inferred in the ionosphere will be in error because it is based on the same T89 model that seemingly incorrectly projects the satellite position to the ionosphere. As mentioned in 2d above, it would be helpful to try to estimate the uncertainty by considering whether there is some simple rescaling of the T89 model that would reduce the discrepancy in the magnetopause-to-ionosphere projection. I would also add that the description of the mapping method given in lines 372-376 is too vague to allow others to reproduce your method. It also seems that you use the

C8

same T89 mapping factor of 55 for all three events, which seems questionable, e.g., solar wind dynamic pressure is 50% larger for Apr 19 event. It also implies that the factor is the same for all MLT which is unlikely I think, especially over the 10 Re magnetopause extent inferred for the Apr 29 event. Please could you improve your method description and assess the associated uncertainties.

Response: We would like to clarify that the T89 model is Kp based and does not have solar wind input. Our events all occurred around Kp=2 and that's why the mapping factor is the about same.

In the new Figure #2 (see attachment), the satellite footprints were mapped within the radar FOV and nearly aligned with the OCB. In the Figure 4 event, the 'outward magnetopause motion' does not appear to be due to IMF or solar wind pressure pulses because neither changed substantially. Local distortions of the magnetopause may be a possibility. In any case, there is no known reliable way to modify the model and thus we choose to take the best estimate from the model. In the Figure 6 case, THE crossed the magnetopause later than THA, and at the time of Figure 6 THE was still inside the magnetosphere. THE footprint later on moved to the OCB as the satellite crossed the magnetopause.

As mentioned above, our study does not concern OCB outside the radar FOV. Although we agree that the OCB could be obtained by model magnetopause mapping or addition of DMSP, it does not affect the reconnection burst extent within the radar FOV.

7. I would recommend that you reference and discuss the following first 5 papers in lines 136-141 as these have done a similar comparison of simultaneous reconnection evidence from space and ground to infer X-line length. I would also recommend that you consider the implications of these and the sixth reference to your discussion in section 3.4 as they seem to be relevant to the factors affecting X-line extent (e.g., IMF orientation, component or anti-parallel reconnection, turbulence): Phan, T.D., Freeman, M.P., Kistler, L.M. et al. *Earth Planet Sp* (2001) 53: 619.

C9

<https://doi.org/10.1186/BF03353281> Pinnock, M., G. Chisham, I. J. Coleman, M. P. Freeman, M. Hairston, and J.-P. Villain (2003), The location and rate of dayside reconnection during an interval of southward interplanetary magnetic field, *Ann. Geophys.*, 21, 1467–1482. Coleman, I. J., G. Chisham, M. Pinnock, and M. P. Freeman (2001), An ionospheric convection signature of antiparallel reconnection, *J. Geophys. Res.*, 106, 28,995–29,007. Chisham, G., I. J. Coleman, M. P. Freeman, M. Pinnock, and M. Lester (2002), Ionospheric signatures of split reconnection X-lines during conditions of IMF Bz < 0 and |By|/|Bz|: Evidence for the antiparallel merging hypothesis, *J. Geophys. Res.*, 107(A10), 1323, doi:10.1029/2001JA009124. Chisham, G., M. P. Freeman, I. J. Coleman, M. Pinnock, M. R. Hairston, M. Lester, and G. Sofko (2004b), Measuring the dayside reconnection rate during an interval of due northward interplanetary magnetic field, *Ann. Geophys.*, 22, 4243–4258. Coleman, I. J., and M. P. Freeman (2005), Fractal reconnection structures on the magnetopause, *Geophys. Res. Lett.*, 32, L03115, doi:10.1029/2004GL021779.

Response: We modify the text in Section 3.4 as “. . .The IMF Bx and By components are known to modify the magnetic shear across the magnetopause and to affect the occurrence location of reconnection. Studies have found that small  $|B_y|/|B_z|$  relates to anti-parallel and large  $|B_y|/|B_z|$  to component reconnection [Coleman et al., 2001; Chisham et al., 2002; Trattner et al., 2007]. Large  $|B_x|/|B|$ , i.e. cone angle, also favors formation of high-speed magnetosheath jets [Archer and Horbury, 2013; Plaschke et al., 2013] of a few Re in scale size, resulting in a turbulent magnetosheath environment for reconnection to occur [Coleman, and Freeman, 2005]”

---

Interactive comment on *Ann. Geophys. Discuss.*, <https://doi.org/10.5194/angeo-2018-63>, 2018.

C10

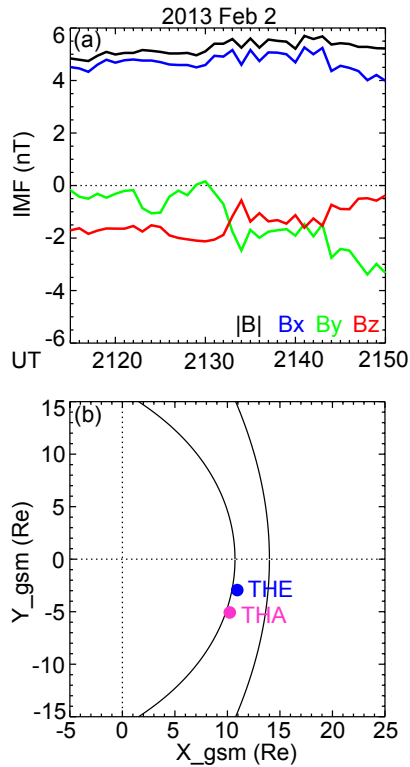


**Fig. 1.** Figure 1a: OMNI IMF condition on Feb 2, 2013. Figure 1b: THE and THA locations projected to the GSM X-Y plane. The inner curve marks the magnetopause and the outer curve marks the bow shock.

C11

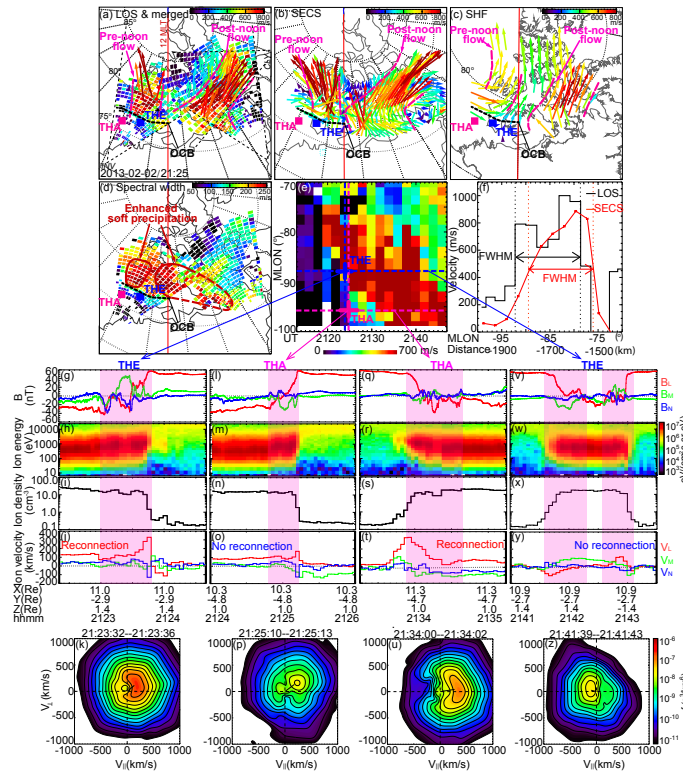


**Fig. 2.** Figure 2a: SuperDARN LOS speeds (color tiles) and merged velocity vectors (color arrows) in the Altitude adjusted corrected geomagnetic (AACGM) coordinates. The FOVs of the RKN, INV, and CLY radars are

C12

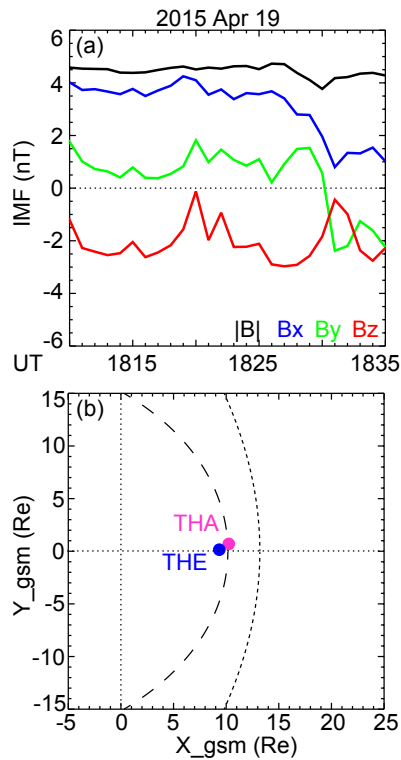


**Fig. 3.** Figure 3: OMNI IMF condition and THEMIS satellite locations on Apr 19, 2015 in a similar format to Figure 1.

C13

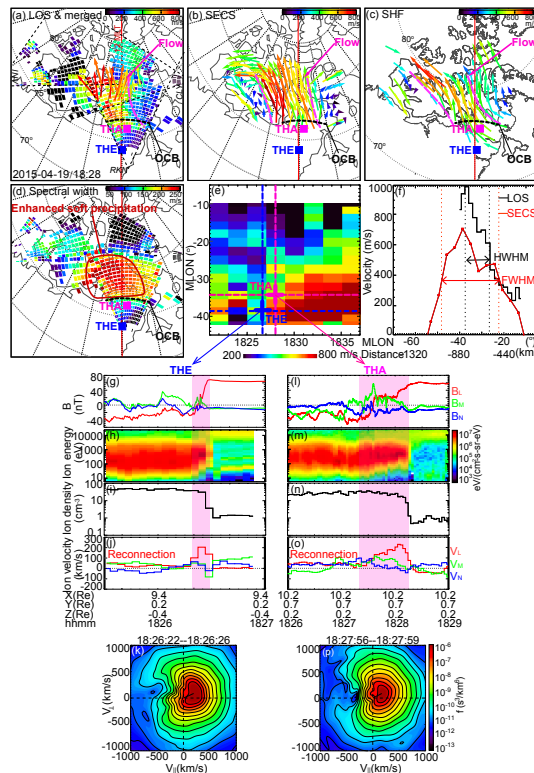


**Fig. 4.** Figure 4. THEMIS and SuperDARN measurements of reconnection bursts on Apr 19, 2015 in a similar format to Figure 2. The velocity time evolution in Figure 4e and the velocity profile in Figure 4f are t

C14

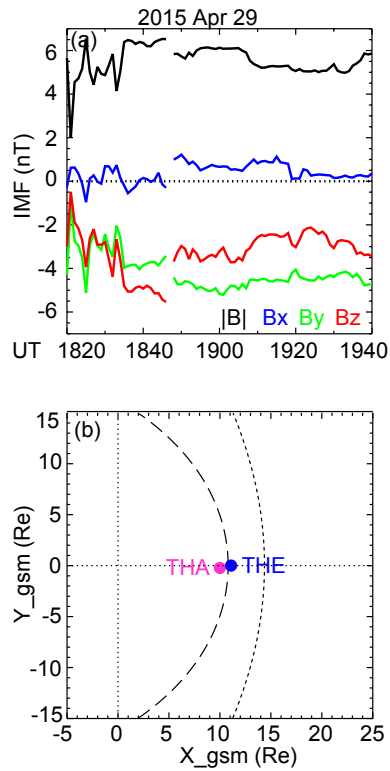


**Fig. 5.** Figure 5. OMNI IMF condition and THEMIS satellite locations on Apr 29, 2015 in a similar format to Figure 1.

C15

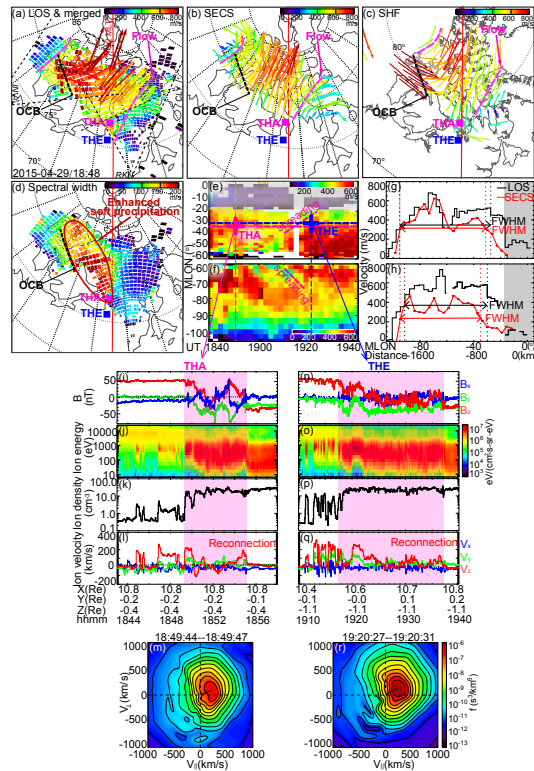


**Fig. 6.** Figures 6a-d: SuperDARN measurements of reconnection bursts on Apr 29, 2015 in a similar format to Figures 2a-d except that in Figure 6a the color of the CLY color tiles represent LOS speeds towards t

C16



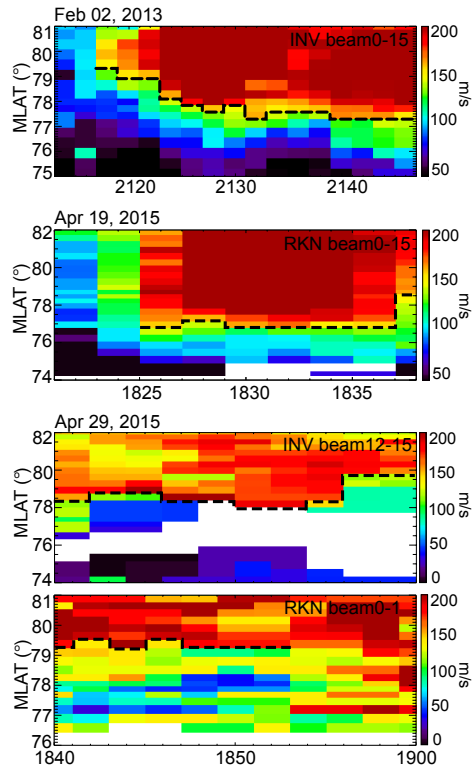


**Fig. 7.** Figure S1. Location of the open-closed field line boundary (marked by the black dashed line) in the three studied events. The open-closed field line boundary is determined based on the spectral width

C17

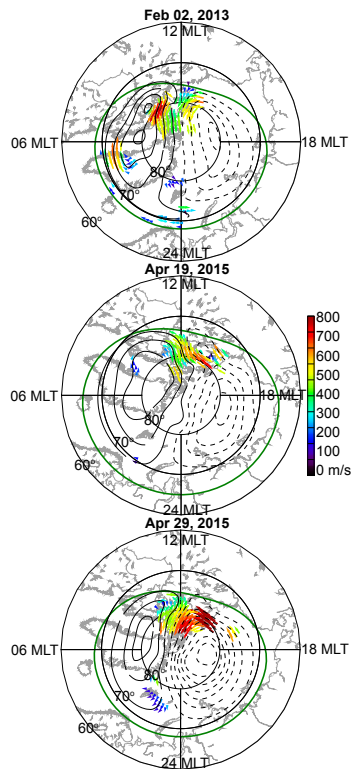


**Fig. 8.** Figure S2. Global convection maps of the three studied events. The SHF velocities are shown as color arrows, and the contours of the electric potential are shown as black solid (at the duskside) and d

C18

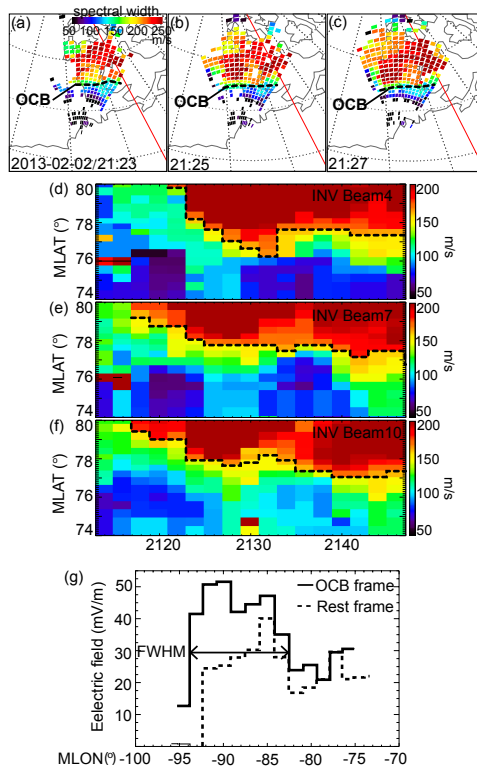


**Fig. 9.** Figure S3. Reconnection electric along the open-closed field line boundary for the Feb 02, 2013 event. Figures S3a-c: snapshots of spectral width measurements around the space-ground conjunction time